## 5. REFERENCES


**Abdallah, A.M. and Abd El-Hady, F.M. (1966):** Geology of Gulf of Suez. U. A. R. J. Geol., 10(1): 1-24.

**Abdallah, M.A. (1993):** Structural geology of the area between El Galala El-Baharyia and GabalAkheider. Ph.D. Thesis, Fac. Sci., Ain Shams Univ., Cairo 199p.

**Barsukov, P.O., Fainberg E.B, and Khabensky E.O., 2004:** Joint inversion of TEM and DC soundings, Near Surface, 10th European Meeting of Environmental and Engineering Geophysics, Utrecht, The Netherlands.

**Ebraheem, A.M., Sensosy, M.M., Dahab, K.A., 1997:** Geoelectrical and Hydro-geochemical studies for delineating ground-water contamination due to salt-water intrusion in the northern part of the Nile delta, Egypt.Ground Water 35, 216– 222.

**EGSMA, (1999):** Geotechnical study and groundwater exploration for the free economic area, northwest Gulf of Suez, Egypt, internal report (in Arabic).

**Fitterman, D.V., Stewart, M.T., 1986:** Transient electromagnetic sounding for groundwater. Geophysics 51, 995– 1005.

**Flathe, H., 1955:** Possibilities and limitations in applying geoelectrical methods to hydrogeological problems in the coastal areas of North West Germany. Geophysical Prospecting 3, 95–110

**Goldman, M., Du Plooy, A. and Evkard, M., 1994:** On reducing ambiguity in the interpretation of transient electromagnetic sounding data. Geophysical Prospecting, 42, 3-25.

**Meju, M.A., 2005:** Simple relative space–time scaling of electrical and electromagnetic depth sounding arrays: implications for electrical static shift removal and joint DC-TEM data in version with the most-squares criterion. Geophysical Prospecting 53 (4), 463–480.

**McNeill, J.D., 1990:** Use of electromagnetic methods for groundwater studies. In: Ward, S.H. (Ed.), Geotechnical and Environmental Geophysics, vol. 1, Review and Tutorial, Society of Exploration Geophysicists Investigations, No. 5, pp. 107–112.

**Spies, B.R. 1983:** Recent developments in the use of surface electricalmethods for oil and gas exploration in the Soviet Union. Geophysics 48,1102–1112.

**Urish, D.W., Frohlich, R.K., 1990:** Surface electrical resistivity in coastal groundwater exploration. Geoexploration 26, 267–289.

**Van Overmeeren, R.A., 1989:** Aquifer boundaries explored by geoelectrical measurements in the coastal plain of Yemen: a case of equivalence. Geophysics 54, 38-48.

**Zohdy, A.A.R., 1969:** The use of Schlumberger and equatorial soundings in ground-water investigations near El Paso, Texas. Geophysics 34, 713–728.


*Egyptian Geophysical Society*
*EGS Journal, Vol. 12, No. 1, 41-48 (2014)*

# IMPACT OF THE PLATE MOTION ON THE DEFORMATION ANALYSIS OF CAIRO NETWORK: CASE STUDY WITH SIMULATED DATA

A.S. Mohamed*, A. Mousa*, B. Laszlo**,
A.A. Nadia*, R. Ali* and H. Khalil*

** National Research Institute of Astronomy and Geophysics, Helwan, Egypt*
*** Research Centre for Astronomy and Earth Sciences, Sopron, Hungary*

## تأثير الصفيحة التكتونية على التشوهات المحلية فى شبكة القاهرة الإقليمية: دراسة حالة مع المماثلة

**الخلاصـــة:** يتعرض هذا البحث بالمناقشة والتحليل لطريقة ضبط خطوط القاعدة مصحوبةً بالتحويل المتماثل للإحداثيات كطريقة بديلة لضبط وتدقيق شبكة القاهرة الإقليمية وذلك بهدف تقييم وتعيين قيم معدلات التشوهات المحلية (البينية) في الصفيحة التكتونية والتي توجد فيها منطقة القاهرة. وقد أكدت النتائج المستخلصة من البحث أن الطريقة المستخدمة لها فعالية مميزة وذات قدرة على حساب التغير في الإحداثيات ومعدل معاملات الدوران العالمية ومعامل المقياس وذلك في خطوة واحدة. ولهذا فقد تم استخدام الطريقة الجديدة لدراسة تأثير الحركة التكتونية العالمية على نتائج تلك الشبكات الإقليمية. ومن هذا المنطلق فقد قام الباحثون بالاستعانة ببيانات محاكاة للتحركات المتوقعة من نتائج رصد شبكة القاهرة الجيوديسية الإقليمية. وقد أظهرت نتائج حساب تحركات الصفيحة التكتونية في ظل وجود محاكاة خطأ معامل المقياس (الناشئ عن خطأ نمذجة تأثير الغلاف الجوي علي أرصاد النظام العالمي لتحديد الإحداثيات المعروف بنظام GPS) وكذلك الأخطاء العشوائية بأنه يجب أخذ تأثير الحركة التكتونية العالمية على نتائج رصد شبكة القاهرة الإقليمية في الإعتبارعلي أن تكون الفترة الزمنية للدراسة في حدود العشر سنوات أو أكثر.

**ABSTRACT:** *Integrated baseline adjustment and similarity transformation method is proposed as an alternative strategy for the regional size Cairo Network to estimate intra-plate deformations using GPS observations. The new proposed method is demonstrated to estimate coordinate changes, global rotations and scale parameters in one computational step. The proposed method is used to investigate the significance of the impact of global plate motions on regional crustal movements network. Simulated data of the regional Cairo network is used for this evaluation. The estimated plate motions, simulated scale bias (due to miss-modeling of troposphere effect on GPS data) and baseline noise proved that the impact of plate motions have to be taken into account in the case of Cairo network if the investigation period is near or larger than ten years.*

## INTRODUCTION

Recent crustal movement monitoring was carried out in Cairo region after the earthquake of 12th October 1992 in Dahshour area, 35 km southwest Cairo City center with a magnitude of 5.9. This earthquake was strongly felt over the whole area of Egypt. It caused a widespread damage in Cairo, Giza and El-Faiyum provinces. According to official reports about 8500 dwellings were destroyed, 561 people were killed, 6500 people were injured and the estimated damage is more than 35 million US dollar (Khater 1992, Thenhaus et al., 1993, Youssef et al., 1992).

GPS network was established in 1995 covering Cairo City and the southern part of the Nile Delta. It was selected according to the geological and geophysical considerations taking into account the requirements of GPS technique. The river Nile runs from south to north in the middle of the network. The initial measurements were carried out in 1996. The measurements were repeated once a year until 2007. Abdel-Monem (2005) presented and analyzed the data during the period from 1986 to 2003. Some points of the network were destructed, therefore the network was updated in 2011 and the initial measurements were performed in January 2012 (Abdel-Monem, 2011).

In this study, we used simulation analysis to investigate the impact of global plate motions on the regional size Cairo network using GPS observation technique. It is to be noted here that, even in the case of regional investigations, where we are interested only in the intra-plate changes of the network, it is reasonable to connect the network to the nearest permanent IGS station(s). Taking into account the actual coordinates of the IGS station(s) the consonance with the precise ephemerides is warranted, but the global plate motions of the regional network is also inherited.

It may be disadvantageous if the IGS station(s) are very far from the regional network, they are at different tectonic plates or the network is near to the plate borders In the case of Cairo Network all the three circumstances have to be taken into account. The global motions of the networks determined in different observational epoch are usually subtracted by seven parameter similarity transformations (sometimes combined with estimated plate motions) and the residuals are investigated for intra-plate deformations.

In the case of Cairo network the following alternative approach may be reasonably proposed:

**1-Initial epoch:**

1. adjustment of raw GPS observations together with nearest IGS station(s) and precise ephemerides

(using e.g. Bernese software, the resulted coordinates are treated as preliminary coordinates).

2. independent adjustment of properly selected redundant baselines of GPS network without IGS station(s) (using e.g. Bernese software and coordinates from step 1).
3. network adjustment of baselines (from step 2) so that the squares sum of the coordinate changes (with respect to step 1) is minimized (these will be the reference coordinates of the investigations)

***2-i-th epoch*:**

1. the same as initial epoch step1.
2. the same as initial epoch step2.
3. network adjustment of baselines (from step 2) so that the squares sum of the coordinate changes (with respect to step 3 of initial epoch) is minimized (if it is necessary simultaneously estimate the global rotations and scale parameter, too).

The proposed method is tested using simulation data of Cairo network. The result of the proposed technique is compared with the traditional analysis techniques using similarity seven transformation parameters results. It is found that the proposed technique is suitable and efficient for estimating intra-plate motions of such regional network. Global plate tectonics effect is found to be significant for regional Cairo network and must be dealt with when producing the intra-plate motion.

## 1. Methodology and Test Computations

The sketch of the Cairo Network and the properly selected redundant baselines are presented in figure (1). Those baselines that are longer than the radial line 200-600 are not selected. The baseline lengths are between 22 and 69 kilometers.

The coordinates of the *initial epoch* and their estimated changes providing the *i-th epoch* coordinates are given in Table (1). The coordinate changes for ten years period are computed by the UNAVCO plate motion calculator using the "ITRF2000D&A" model (Drewes and Angermann , 2001), which estimates the coordinate changes in three Cartesian components (web of UNAVCO plate motion calculator, 2012).

Figure (2) shows the horizontal changes of the network points due to plate motion in ten years as simulated using the above model. The north components are 0.1697 ±0.0006 m, the east components are 0.2455 ±0.0005 m, and there are no height changes.

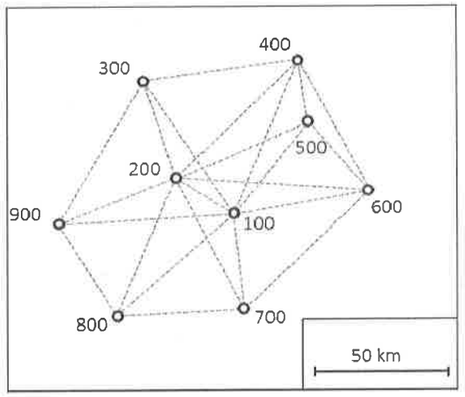


**Figure (1): The sketch of Cairo Network and selected baselines.**

***Table (1): Simulated motion of the network (m) using ITRF2000 (D&A) model.***

| | *initial epoch* | 10 years plate motion | | | *simulated epoch* |
|---|---|---|---|---|---|
| Stations | *X*<br>*Y*<br>*Z* | *ΔX* | *ΔY* | *ΔZ* | *X*<br>*Y*<br>*Z* |
| 100 | 4728141<br>2879661<br>3157147 | -0.1995 | 0.1661 | 0.1473 | 4728140.8005<br>2879661.1661<br>3157147.1473 |
| 200 | 4733789<br>2858114<br>3168117 | -0.1990 | 0.1663 | 0.1474 | 4733788.8010<br>2858114.1663<br>3168117.1474 |
| 300 | 4723885<br>2839244<br>3199346 | -0.1993 | 0.1658 | 0.1658 | 4723884.8007<br>2839244.1658<br>3199346.1471 |
| 400 | 4692946<br>2882752<br>3205908 | -0.2011 | 0.1647 | 0.1463 | 4692945.7989<br>2882752.1647<br>3205908.1463 |
| 500 | 4700632<br>2891947<br>3186688 | -0.2008 | 0.1650 | 0.1465 | 4700631.7992<br>2891947.1650<br>3186688.1465 |
| 600 | 4700712<br>2917884<br>3163657 | -0.2011 | 0.1651 | 0.1466 | 4700711.7989<br>2917884.1651<br>3163657.1466 |
| 700 | 4742146<br>2889985<br>3126746 | -0.1990 | 0.1667 | 0.1477 | 4742145.8010<br>2889985.1667<br>3126746.1477 |
| 800 | 4767118<br>2851785<br>3123591 | -0.1975 | 0.1676 | 0.1484 | 4767117.8025<br>2851785.1676<br>3123591.1484 |
| 900 | 4762265<br>2826732<br>3153862 | -0.1975 | 0.1674 | 0.1482 | 4762264.8025<br>2826732.1674<br>3153862.1482 |
| mean<br>stand. dev. | | -0.1994<br>0.0015 | 0.1661<br>0.0011 | 0.1473<br>0.0008 | |



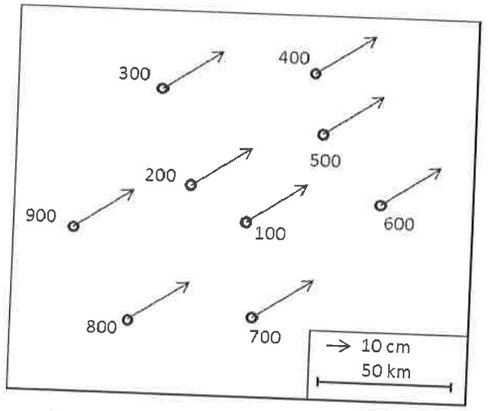


**Figure (2): The estimated horizontal plate motions for the ten years.**

To convert the three components of the plate motions into the rotations about the coordinate axes the well-known seven parameter similarity transformation is applied ( e.g. Spath, 2004):

$$\begin{bmatrix} X \\ Y \\ Z \end{bmatrix}_{II} = \begin{bmatrix} X \\ Y \\ Z \end{bmatrix}_{I} + \begin{bmatrix} 1 & 0 & 0 & 0 & -Z/\rho & Y/\rho & X/10^6 \\ 0 & 1 & 0 & Z/\rho & 0 & -X/\rho & Y/10^6 \\ 0 & 0 & 1 & -Y/\rho & X/\rho & 0 & Z/10^6 \end{bmatrix}_{I} \begin{bmatrix} t_x \\ t_y \\ t_z \\ R_x \\ R_y \\ R_z \\ sc \end{bmatrix} \quad (1)$$

where $t_x$, $t_y$, $t_z$ are the translations, $R_x$, $R_y$, $R_z$ are the rotations, $sc$ is a scale parameter (the difference from unity) and $\rho = 206264.8$ arcsec. If the coordinates are in meter the rotations are given in arcsec and the $sc$ is in ppm. The subscripts *I* and *II* distinguish the two coordinate systems. In the case of equation (1) the system I is shifted, rotated and scaled to fit into system II.

The least-squares adjustment of the observational equations (1) can be used to estimate the seven parameters in the global coordinate system. If the coordinates are shifted to the center of gravity the alternative solution can be computed directly as:

$$dx = X_{II} - X_I, \quad dy = Y_{II} - Y_I, \quad dz = Z_{II} - Z_I,$$

$$t_x = \frac{\sum dx}{n}, \quad t_y = \frac{\sum dy}{n}, \quad t_z = \frac{\sum dz}{n},$$

$$R_x = \frac{\sum(Z_{Ic} d_y - Y_{Ic} d_z)}{\sum(Z_{Ic}^2 + Y_{Ic}^2)}, \quad R_y = \frac{\sum(-Z_{Ic} d_x + X_{Ic} d}{\sum(Z_{Ic}^2 + X_{Ic}^2)}$$

$$R_z = \frac{\sum(Y_{Ic} d_x - X_{Ic} d_y)}{\sum(Y_{Ic}^2 + X_{Ic}^2)}, \quad (2)$$

$$sc = \frac{\sum(X_{Ic} d_x + Y_{Ic} d_y + Z_{Ic} d_z)}{\sum(X_{Ic}^2 + Y_{Ic}^2 + Z_{Ic}^2)},$$

where $n$ is a number of included stations and the subscript *Ic* refer to the coordinates in shifted system. In the case of the presented transformations the input coordinates are treated by using equal unit weights.

For the new proposed method, the effects of the transformation on the GPS derived baseline components for stations i and j can be modeled using equation (1) as:

$$\begin{bmatrix} \Delta X_{ij} \\ \Delta Y_{ij} \\ \Delta Z_{ij} \end{bmatrix}_{II} =$$

$$\begin{bmatrix} 1 & 0 & 0 & -1 & 0 & 0 & 0 & -(Z_i - Z_j)/\rho \\ 0 & 1 & 0 & 0 & -1 & 0 & (Z_i - Z_j)/\rho & 0 \\ 0 & 0 & 1 & 0 & 0 & -1 & -(Y_i - Y_j)/\rho & (X_i - X_j)/\rho \end{bmatrix}$$

$$\begin{bmatrix} (Y_i - Y_j)/\rho & (X_i - X_j)/10^6 \\ (X_i \quad X_j)/\rho & (Y_i - Y_j)/10^6 \\ 0 & (Z_i - Z_j)/10^6 \end{bmatrix}_I \begin{bmatrix} dx_i \\ dy_i \\ dz_i \\ dx_j \\ dy_j \\ dz_j \\ R_x \\ R_y \\ R_z \\ sc \end{bmatrix} \quad (3)$$

where the right hand side is composed of the initial coordinates and $(dx, dy, dz)$ are the unknown coordinate changes.

The system of equations (3) can be used as the extended observation equations of the least-square adjustment including global rotations and scale parameter. In this case the equations contain three translational defects, three rotational defects and one scale defect. The singularities can be handled according to equation (2) by seven constraint equations:

$$\sum d_x = 0, \quad \sum d_y = 0, \quad \sum d_z = 0,$$

$$\sum(Z_{Ic} d_y - Y_{Ic} d_z) = 0, \quad \sum(-Z_{Ic} d_x + X_{Ic} d_z) = 0,$$

$$\sum(Y_{Ic} d_x - X_{Ic} d_y) = 0, \quad (4)$$

$$\sum(X_{Ic} d_x + Y_{Ic} d_y + Z_{Ic} d_z) = 0,$$

which force no global translations, no rotations and no scale bias with respects to the initial coordinates, these effects are absorbed by the additional global unknowns. as a results of the above constrains, the resulted coordinate changes describe only the intra-plate deformations of the network. This method is the combined baseline adjustment and similarity transformation in one integrated adjustment step. If no rotations and scale are estimated only the translational constraints have to be used (first row of Eq. 4). The constraints provide a solution similar to the free-network approach (Mierlo, 1980), where the squares sum of coordinate changes is minimized. This procedure was implemented in the baseline adjustment software developed for different purposes (Banyai 1991, 2005).

During the test computations the baseline components are treated as uncorrelated quantities with 1 mm a priori standard deviations. In that case they can be compared to the results of similarity transformations.

## 2. RESULTS AND DISCUSSION

The results of the global and the shifted transformations of the initial epoch (I) and the simulated epoch (II) are given in table (2).

***Table (2): Transformation of ITRF2000 (D&A) motions.***

| Unknown | Global | | Shifted | |
|---|---|---|---|---|
| $t_x$ | 0.0007 | ±0.0019 | -0.1994 | ±0.0000 |
| $t_y$ | -0.0001 | ±0.0018 | 0.1661 | ±0.0000 |
| $t_z$ | -0.0005 | ±0.0002 | 0.1473 | ±0.0000 |
| $R_x$ | 0.0061 | ±0.0001 | -0.0005 | ±0.0002 |
| $R_y$ | -0.0075 | ±0.0001 | 0.0061 | ±0.0001 |
| $R_z$ | 0.0001 | ±0.0001 | -0.0075 | ±0.0001 |
| *sc* | | | 0.0001 | ±0.0001 |

It is evident that the translations and the scale bias should be zero in the case of global similarity transformation. The very small discrepancies are the consequences of the truncations of the plate motion calculator after the fourth decimal digit. In the case of shifted transformation the estimated translations are the same as the mean values computed in table (1). The rotations are the same in both cases.

The changes of the selected baselines (Fig. 1) with respect to the initial values are given in Table (3). The mean changes are practically zeros, but their standard deviations are very similar to the relevant values in Table 1. It shows that the residual plate motions are only few millimeters. To estimate the impact of these residuals the baselines were adjusted without rotations and scale bias (using translational constraints). The coordinate changes are summarized in Table (4). It is very interesting that the residual plate motions are absorbed mainly by the vertical components (Fig. 3), which shows the tilt of the network in the direction of the global motions.

***Table (3): Baseline changes (m) using ITRF2000 (D&A) model***

| Baselines | Length (km) | 10 years changes | | |
|---|---|---|---|---|
| | | ΔX | ΔY | ΔZ |
| 400-500 | 23 | 0.0003 | 0.0003 | 0.0002 |
| 200-100 | 25 | -0.0005 | -0.0002 | -0.0001 |
| 500-600 | 35 | -0.0003 | 0.0001 | 0.0001 |
| 100-700 | 35 | 0.0005 | 0.0006 | 0.0004 |
| 200-300 | 38 | -0.0003 | -0.0005 | -0.0003 |
| 900-800 | 40 | 0.0000 | 0.0002 | 0.0002 |
| 100-500 | 42 | -0.0013 | -0.0011 | -0.0008 |
| 200-900 | 45 | 0.0015 | 0.0011 | 0.0008 |
| 800-700 | 46 | -0.0015 | -0.0009 | -0.0007 |
| 100-600 | 47 | -0.0016 | -0.0010 | -0.0007 |
| 200-500 | 51 | -0.0018 | -0.0013 | -0.0009 |
| 200-700 | 53 | 0.0000 | 0.0004 | 0.0003 |
| 300-400 | 54 | -0.0018 | -0.0011 | -0.0008 |
| 400-600 | 55 | 0.0000 | 0.0004 | 0.0003 |
| 200-800 | 56 | 0.0015 | 0.0013 | 0.0010 |
| 100-800 | 59 | 0.0020 | 0.0015 | 0.0011 |
| 100-300 | 59 | 0.0002 | -0.0003 | -0.0002 |
| 100-400 | 60 | -0.0016 | -0.0014 | -0.0010 |
| 300-900 | 61 | 0.0018 | 0.0016 | 0.0011 |
| 200-400 | 61 | -0.0021 | -0.0016 | -0.0011 |
| 600-700 | 62 | 0.0021 | 0.0016 | 0.0011 |
| 100-900 | 63 | 0.0020 | 0.0013 | 0.0009 |
| 200-600 | 68 | -0.0021 | -0.0012 | -0.0008 |
| mean | 49 | -0.0001 | 0.0000 | 0.0000 |
| stand. dev. | 12 | 0.0014 | 0.0011 | 0.0008 |

***Table (4): Coordinate changes (m) after baseline adjustment without rotations and scale bias caused by plate motion***

| Stations | North | East | Up |
|---|---|---|---|
| 100 | 0.0000 | 0.0001 | -0.0000 |
| 200 | -0.0001 | -0.0000 | 0.0005 |
| 300 | -0.0001 | -0.0003 | -0.0001 |
| 400 | 0.0002 | -0.0003 | -0.0023 |
| 500 | 0.0002 | -0.0002 | -0.0019 |
| 600 | 0.0004 | 0.0001 | -0.0020 |
| 700 | 0.0000 | 0.0003 | 0.0008 |
| 800 | -0.0002 | 0.0003 | 0.0027 |
| 900 | -0.0004 | 0.0002 | 0.0025 |
| mean | 0.0000 | 0.0000 | 0.0000 |
| stand. dev. | 0.0002 | 0.0002 | 0.0018 |



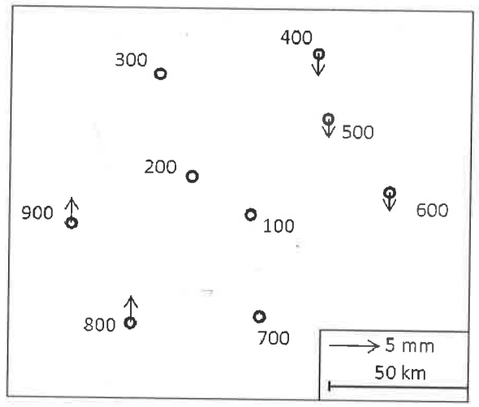


**Figure (3): Estimated vertical motions as the impact of residual plate motions.**

The similarity transformation was repeated using the newly adjusted coordinates, where the mean changes had already been cancelled by the network adjustment. The surprising result can be found in Table (5). The network preserved the translational and rotational features of the plate motions. In the global model the translations are preserved in millimeter level, but with different signs. The combined adjustment with rotations and scale bias provided the same rotations and scale parameters as the similarity transformations.

***Table (5): Transformation of adjusted network after baseline adjustment without rotations and scale bias caused by plate motion***

| Unknown | Global | Shifted |
|---|---|---|
| $t_x$ | 0.1981 ±0.0014 | -0.0000 ±0.0000 |
| $t_y$ | -0.1654 ±0.0019 | -0.0000 ±0.0000 |
| $t_z$ | -0.1474 ±0.0018 | -0.0000 ±0.0000 |
| $R_x$ | -0.0005 ±0.0002 | -0.0005 ±0.0002 |
| $R_y$ | 0.0061 ±0.0001 | 0.0061 ±0.0001 |
| $R_z$ | -0.0075 ±0.0001 | -0.0075 ±0.0001 |
| *sc* | 0.0001 ±0.0001 | 0.0001 ±0.0001 |

During the adjustment of raw GPS observations the not properly modeled atmospheric effects may cause a scale bias, as well. To study the effects of small 0.05 ppm scale bias a new data set was simulated (Table 6). The magnitude of the standard deviations is similar to the plate motion residuals. The change of the baselines reflects only scale effects. The results of the baseline adjustment without rotations and scale bias (using translational constraints) are given in Table (7).

***Table (6): Baseline changes (m) caused by scale bias.***

| Baselines | Length (km) | 0.05 ppm | | |
|---|---|---|---|---|
| | | ΔX | ΔY | ΔZ |
| 400-500 | 23 | 0.0004 | 0.0005 | -0.0010 |
| 200-100 | 25 | -0.0003 | 0.0011 | -0.0005 |
| 500-600 | 35 | 0.0000 | 0.0013 | -0.0012 |
| 100-700 | 35 | 0.0007 | 0.0005 | -0.0015 |
| 200-300 | 38 | -0.0005 | -0.0009 | 0.0016 |
| 900-800 | 40 | 0.0002 | 0.0013 | -0.0015 |
| 100-500 | 42 | -0.0014 | 0.0006 | 0.0015 |
| 200-900 | 45 | 0.0014 | -0.0016 | -0.0007 |
| 800-700 | 46 | -0.0012 | 0.0019 | 0.0002 |
| 100-600 | 47 | -0.0014 | 0.0019 | 0.0003 |
| 200-500 | 51 | -0.0017 | 0.0017 | 0.0009 |
| 200-700 | 53 | 0.0004 | 0.0016 | -0.0021 |
| 300-400 | 54 | -0.0015 | 0.0022 | 0.0003 |
| 400-600 | 55 | 0.0004 | 0.0018 | -0.0021 |
| 200-800 | 56 | 0.0017 | -0.0003 | -0.0022 |
| 100-800 | 59 | 0.0019 | -0.0014 | -0.0017 |
| 100-300 | 59 | -0.0002 | -0.0020 | 0.0021 |
| 100-400 | 60 | -0.0018 | 0.0002 | 0.0024 |
| 300-900 | 61 | 0.0019 | -0.0006 | -0.0023 |
| 200-400 | 61 | -0.0020 | 0.0012 | 0.0019 |
| 600-700 | 62 | 0.0021 | -0.0014 | -0.0018 |
| 100-900 | 63 | 0.0017 | -0.0026 | -0.0002 |
| 200-600 | 68 | -0.0017 | 0.0030 | -0.0002 |
| mean | 49 | 0.0000 | 0.0004 | -0.0003 |
| stand. dev. | 12 | 0.0014 | 0.0015 | 0.0015 |

***Table (7): Coordinate changes (m) after baseline adjustment without rotations and scale caused by 0.05 ppm scale bias***

| Stations | North | East | Up |
|---|---|---|---|
| 100 | -0.0004 | 0.0004 | 0.0000 |
| 200 | 0.0002 | -0.0007 | 0.0000 |
| 300 | 0.0020 | -0.0013 | 0.0000 |
| 400 | 0.0024 | 0.0014 | 0.0000 |
| 500 | 0.0012 | 0.0016 | 0.0000 |
| 600 | -0.0001 | 0.0027 | 0.0000 |
| 700 | -0.0022 | 0.0004 | 0.0000 |
| 800 | -0.0024 | -0.0018 | 0.0000 |
| 900 | -0.0007 | -0.0028 | 0.0000 |
| mean | 0.0000 | 0.0000 | 0.0000 |
| stand. dev. | 0.0017 | 0.0018 | 0.0000 |

Contrary to the plate motions the vertical changes are zeros. The horizontal changes are shown in figure (4). The transformation of the new coordinates is given in Table (8). Both transformations preserved the zero rotations and the simulated scale bias. However the translations of the global solution compensate only the fact that global coordinates are scaled which shift the stations further from the global center.

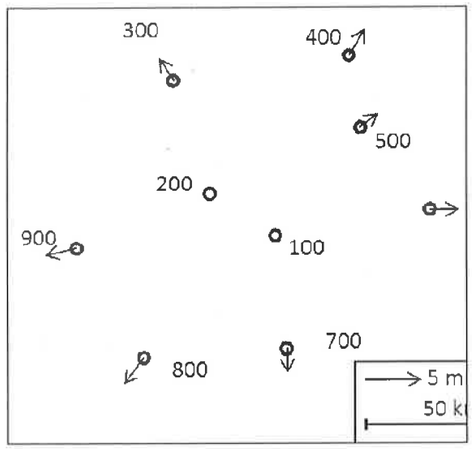


**Figure (4): Estimated horizontal motions as the impact of 0.05 ppm scale bias.**

*Table (8): Transformation of adjusted network after baseline adjustment without rotations and scale caused by 0.05 ppm scale bias*

| Unknown | Global | | Shifted | |
|---|---|---|---|---|
| $t_x$ | -0.2372 | ±0.0016 | -0.0000 | ±0.0000 |
| $t_y$ | -0.1423 | ±0.0021 | 0.0000 | ±0.0000 |
| $t_z$ | -0.1574 | ±0.0020 | -0.0000 | ±0.0000 |
| $R_x$ | -0.0000 | ±0.0001 | -0.0000 | ±0.0002 |
| $R_y$ | -0.0000 | ±0.0001 | -0.0000 | ±0.0001 |
| $R_z$ | 0.0000 | ±0.0001 | 0.0000 | ±0.0001 |
| *sc* | 0.0499 | ±0.0002 | 0.0499 | ±0.0001 |

The baselines composed from the sum of plate motion and the additional scale bias was also adjusted at the same way as before. The results are summarized in tables 9 and 10. It is not surprising that the sum of tables 4 and 7 is very similar to table 9. Therefore the figures 3 and 4 are valid in this case, too. Both transformations are provided the same rotations and scales, but the translations are the combinations of rotation and scale effects. The discrepancies are a little bit worse because of the additional numerical truncations of the scale effects.

In the previous investigations only the numerical truncations were the only error sources of the simulated baselines. In the next investigations normally distributed residuals ($N(0,1)$ mm) were added to the baseline components. Consequently they contain plate motions, scale bias and white noise as well. The baseline residuals are given in table 11.

*Table (9): Coordinate changes (m) after baseline adjustment without rotations and scale caused by plate motion and scale bias.*

| Stations | North | East | Up |
|---|---|---|---|
| 100 | -0.0004 | 0.0004 | -0.0000 |
| 200 | 0.0000 | -0.0007 | 0.0005 |
| 300 | 0.0019 | -0.0016 | -0.0001 |
| 400 | 0.0026 | 0.0011 | -0.0023 |
| 500 | 0.0014 | 0.0014 | -0.0019 |
| 600 | 0.0003 | 0.0028 | -0.0020 |
| 700 | -0.0022 | 0.0007 | 0.0008 |
| 800 | -0.0026 | -0.0015 | 0.0027 |
| 900 | -0.0010 | -0.0026 | 0.0025 |
| mean | 0.0000 | 0.0000 | 0.0000 |
| stand. dev. | 0.0018 | 0.0017 | 0.0018 |

*Table (10): Transformation of adjusted network after baseline adjustment without rotations and scale caused by plate motion and scale bias*

| unknown | global | | shifted | |
|---|---|---|---|---|
| $t_x$ | -0.0405 | ±0.0021 | -0.0000 | ±0.0000 |
| $t_y$ | -0.3131 | ±0.0027 | 0.0000 | ±0.0000 |
| $t_z$ | -0.3056 | ±0.0026 | -0.0000 | ±0.0000 |
| $R_x$ | -0.0004 | ±0.0001 | -0.0004 | ±0.0001 |
| $R_y$ | 0.0061 | ±0.0001 | 0.0061 | ±0.0001 |
| $R_z$ | -0.0076 | ±0.0001 | -0.0076 | ±0.0001 |
| *sc* | 0.0507 | ±0.0003 | 0.0507 | ±0.0003 |

The baselines were adjusted without rotations and scale bias (using translational constraints). The coordinate changes and the transformations are summarized in tables 12 and 13. The difference between tables 13 and 10 shows the effect of the simulated random noise.

The adjustment was repeated by the combined baseline adjustment and similarity transformation (Eq. 3 and 4). The results can be found in table 14. Comparing tables 13 and 14, it can be concluded that the combined adjustment provided the same parameters.

In the next investigation the plate motions of stations 400, 500 and 600 were reduced by 10 percent to simulate single station movements. During the combined adjustment these station were not included in the derivation of the constraint equation (4). It means that the network is rotated about a new center. All the baselines are rotated and scaled, but the neglected stations are allowed to change freely (not involved in the minimum norm). The results are given in table 15. The small changes with respect to table 14 prove that the rotations, scale and single station movements were properly preserved, in spite of the fact that the large number of baseline connected to the three stations were not involved in the estimation of global parameters.



*Table (11): Baseline changes (m) caused by plate motions, 0.05 ppm scale bias and N(0,1) mm noise.*

| Baselines | Length (km) | Combined | | |
|---|---|---|---|---|
| | | ΔX | ΔY | ΔZ |
| 400-500 | 23 | 0.0008 | 0.0004 | -0.0014 |
| 200-100 | 25 | -0.0009 | -0.0013 | -0.0010 |
| 500-600 | 35 | -0.0006 | 0.0013 | -0.0011 |
| 100-700 | 35 | 0.0020 | 0.0007 | -0.0029 |
| 200-300 | 38 | -0.0005 | -0.0012 | 0.0042 |
| 900-800 | 40 | 0.0001 | 0.0015 | -0.0016 |
| 100-500 | 42 | -0.0045 | 0.0010 | 0.0012 |
| 200-900 | 45 | 0.0015 | -0.0001 | 0.0008 |
| 800-700 | 46 | -0.0022 | 0.0018 | 0.0004 |
| 100-600 | 47 | -0.0038 | 0.0012 | 0.0001 |
| 200-500 | 51 | -0.0029 | 0.0010 | -0.0014 |
| 200-700 | 53 | -0.0011 | 0.0032 | -0.0037 |
| 300-400 | 54 | -0.0046 | 0.0008 | -0.0002 |
| 400-600 | 55 | 0.0025 | 0.0024 | -0.0014 |
| 200-800 | 56 | 0.0020 | 0.0014 | -0.0013 |
| 100-800 | 59 | 0.0047 | 0.0008 | 0.0007 |
| 100-300 | 59 | -0.0003 | -0.0033 | 0.0008 |
| 100-400 | 60 | -0.0038 | -0.0016 | 0.0012 |
| 300-900 | 61 | 0.0038 | 0.0002 | 0.0008 |
| 200-400 | 61 | -0.0043 | -0.0001 | 0.0003 |
| 600-700 | 62 | 0.0028 | 0.0000 | -0.0014 |
| 100-900 | 63 | 0.0048 | -0.0013 | 0.0011 |
| 200-600 | 68 | -0.0037 | 0.0028 | -0.0001 |
| mean | 49 | -0.0003 | 0.0005 | -0.0002 |
| stand. dev. | 12 | 0.0030 | 0.0015 | 0.0016 |

*Table (12): Coordinate changes (m) after baseline adjustment without rotations and scale caused by plate motions, 0.05 ppm scale bias and N(0,1) mm noise.*

| Stations | North | East | Up |
|---|---|---|---|
| 100 | -0.0003 | 0.0001 | -0.0001 |
| 200 | -0.0001 | -0.0011 | 0.0007 |
| 300 | 0.0018 | -0.0018 | 0.0001 |
| 400 | 0.0028 | 0.0014 | -0.0028 |
| 500 | 0.0011 | 0.0018 | -0.0020 |
| 600 | 0.0002 | 0.0029 | -0.0014 |
| 700 | -0.0029 | 0.0011 | 0.0004 |
| 800 | -0.0025 | -0.0014 | 0.0025 |
| 900 | -0.0002 | -0.0029 | 0.0029 |
| mean | 0.0000 | 0.0000 | 0.0000 |
| stand. dev. | 0.0018 | 0.0019 | 0.0019 |

*Table (13): Transformation of adjusted network after baseline adjustment without rotations and scale caused by plate motions,0.05 ppm scale bias and N(0,1) mm noise.*

| Unknown | Global | | Shifted | |
|---|---|---|---|---|
| $t_x$ | -0.0532 | ±0.0192 | -0.0000 | ±0.0001 |
| $t_y$ | -0.3294 | ±0.0256 | -0.0000 | ±0.0001 |
| $t_z$ | -0.3135 | ±0.0247 | -0.0000 | ±0.0001 |
| $R_x$ | 0.0002 | ±0.0008 | 0.0002 | ±0.0001 |
| $R_y$ | 0.0063 | ±0.0007 | 0.0063 | ±0.0001 |
| $R_z$ | -0.0075 | ±0.0008 | -0.0075 | ±0.0001 |
| *sc* | 0.0539 | ±0.0027 | 0.0539 | ±0.0027 |

*Table (14): Coordinate changes (m) and estimated parameters after baseline adjustment with integrated model caused by plate motion, 0.05 ppm scale bias and N(0,1) mm noise.*

| Stations | North | East | Up |
|---|---|---|---|
| 100 | 0.0001 | -0.0003 | -0.0001 |
| 200 | -0.0002 | -0.0004 | 0.0002 |
| 300 | -0.0002 | -0.0003 | 0.0001 |
| 400 | 0.0002 | 0.0001 | -0.0005 |
| 500 | -0.0004 | 0.0002 | -0.0001 |
| 600 | 0.0001 | -0.0001 | 0.0007 |
| 700 | -0.0005 | 0.0005 | -0.0004 |
| 800 | 0.0002 | 0.0003 | -0.0002 |
| 900 | 0.0007 | 0.0000 | 0.0003 |
| mean | 0.0000 | 0.0000 | 0.0000 |
| stand. dev. | 0.0004 | 0.0003 | 0.0004 |
| $R_x$ | 0.0002 | ±0.0012 | arcsec |
| $R_y$ | 0.0063 | ±0.0012 | arcsec |
| $R_z$ | -0.0076 | ±0.0012 | arcsec |
| *sc* | 0.0539 | ±0.0012 | ppm |

*Table (15): Coordinate changes (m) and estimated parameters after baseline adjustment with integrated model caused by plate motion, 0.05 ppm scale bias, N(0,1) mm noise and single movement of station 400, 500 and 600.*

| Stations | North | East | Up |
|---|---|---|---|
| 100 | 0.0001 | -0.0003 | 0.0001 |
| 200 | -0.0002 | -0.0003 | 0.0002 |
| 300 | -0.0002 | -0.0002 | -0.0002 |
| 400 | **-0.0168** | **-0.0244** | **-0.0005** |
| 500 | **-0.0173** | **-0.0243** | **0.0000** |
| 600 | **-0.0168** | **-0.0246** | **0.0010** |
| 700 | -0.0006 | 0.0005 | -0.0001 |
| 800 | 0.0002 | 0.0003 | -0.0001 |
| 900 | 0.0007 | 0.0000 | 0.0001 |
| mean* | 0.0000 | 0.0000 | 0.0000 |
| stand. dev. | 0.0004 | 0.0003 | 0.0002 |
| $R_x$ | 0.0010 | ±0.0014 | arcsec |
| $R_y$ | 0.0057 | ±0.0015 | arcsec |
| $R_z$ | -0.0088 | ±0.0017 | arcsec |
| *sc* | 0.0533 | ±0.0017 | ppm |

** without stations 400, 500 and 600.*

## 3. SUMMARY AND CONCLUSIONS

According to the geographic settings and the lack of near IGS stations an alternative procedure was demonstrated for the Cairo network to determine the intra-plate changes without global plate motions. This procedure involves the baseline adjustment and similarity transformation in one integrated computational step.

Simulated global plate motions, additional scale bias (0.05 ppm) and random errors of the baseline components ($\sigma$ =1 mm) were used in the test computations. The global motions were converted to global rotations about the Cartesian coordinate axes.

Estimating 10 years plate motion (UNAVCO calculator, ITRF2000 D&A 2001 model) the selected GPS baseline components (22-69 km) contain only a few mm plate motion residuals. The usual adjustment of the baseline components (using translational constraints) presented only mm level changes mainly in the vertical component. However the similarity transformation proved that these small changes preserved the characteristics of the global plate motions.

The baseline residuals of the simulated scale bias are also in a few mm level. Contrary to the plate motion the network adjustment presented only small horizontal coordinate changes.

In spite of that, the simulated random errors are comparable to the residual plate motions and scale biases of the adjusted network preserved the simulated global effects. These global effects can be handled very efficiently using the presented integrated adjustment model.

In the case of significantly smaller time periods or in the case of significantly smaller networks the baseline residuals caused by global plate motions may be significantly smaller than the noise level of the estimated baselines. In that case there is no need for additional parameters, however, if the similarity transformations or the combined adjustments indicate significant biases, the sources of these biases can be found in the adjustment procedure or in the quality of the raw GPS observations.

In the case of Cairo Network it is reasonable to estimate the impact of the global plate motions during longer investigational periods. The proposed strategy and the integrated adjustment should be tested using real observations as one of the possible option.

## ACKNOWLEDGEMENT

This study was carried out under the scientific cooperation agreement between the National Research Institute of Astronomy and Geophysics, Helwan, Egypt and the Research Centre for Astronomy and Earth Sciences, Sopron, Hungary.

## REFERENCES

**Abdel-Monem, S.M. (2005):** Using compiled seismic and GPS data for hazard estimation in Egypt. NRIAG, Journal of Geophysics, Vol.4, No. 1, pp. 51-79.

**Abdel-Monem, S.M. (2011):** Collaborative Research Project between Egyptian and Hungariann Acadimes (2012-2014) under the title Recent geo-dynamic investigations using geodetic methods

**Bányai, L. (1991):** Treatment of rotation errors in the final adjustment of GPS baseline components. Bull. Geod. 65 , pp 102- 108

**Bányai, L. (2005):** Investigation of GPS antenna mean phase centre offsets using a full roving observation strategy. Journal of Geodesy 79 , pp. 222- 230.

**Drewes, H. and D. Angermann (2001):** The Actual Plate Kinematic and Crustal Deformation Model 2000 (APKIM2000) as a Geodetic Reference System,AIG 2001 Scientific Assembly, Budapest, 2-8 Sept 2001.

**Khater, M. (1992):** Reconnaissance Reporton the Cairo, EgyptEarthquake of October 12, 1992. TechnicalRept. NCEER-92-0033, SUNY-Buffalo, Buffalo, NY, December.

**Mierlo, J. Van (1980):** Free network adjustment and S-transformations. DGK Reiche B, 252.

**Spath, H. (2004):** A numerical method for determining the spatial HELMERT transformation in the case of di_erent scale factors, Zeitschrift fur Vermessungswesen 129, pp. 255-259.

**Thenhaus, P.C., Sharp, R.V., Celebi, M., Ibrahim, A.B.K. and Van, H. (1993):** Reconnaissance Report on the 12 October 1992 Dahshur, Egypt. Earthquake. U.S. GeologicalSurvey, Open-FileReport 93-181, Golden, CO.

**Web of UNAVCO** plate motion calculator: http://www.unavco.org/community_science/science-support/crustal_motion/dxdt/model.html, Last visited December, 2012.

**Youssef, N., Adham, S., Celebi, M. and Malilay, J., (1992):** Cairo, Egypt, Earthquake of October 12. 1992, EERI Newsletter, Vol. 26, No.12, December.

*Egyptian Geophysical Society*
*EGS Journal, Vol. 12, No. 1, 49-64 (2014)*

# PETROPHYSICAL EVALUATION OF SHALY SAND RESERVOIRS USING CMR TOOL IN OFFSHORE SEQUOIA FIELD, NILE DELTA, EGYPT

N.M.H. Abou Ashour, A. Mahmoud and H.M. Mahmoud

** Geophysics Dept., Fac. of Sc., Ain Shams University , Egypt.*

## التقييم البتروفيزيائى لخزانات الحجر الرملى الطفلى باستخدام تسجيلات الرنين المغناطيسى النووى لحقل سيكويا- دلتا النيل - مصر

**الخلاصة:** يختص هذا العمل بدراسة الخصائص البتروفيزيائية وعمل تحليل للمحتوى الهيدروكربوني (الغاز) وبناء نموذج مناسب لخزان سيكويا الحجر الرملى الطفلى لمتكون الوسطانى من البليوسين الواقع فى المنطقة البحرية العميقة لغرب دلتا النيل, مصر. حيث تم حساب المسامية والنفاذية والتشبع بالماء و محتوى الغاز أيضاً اعتماداً على دراسة البيانات المتاحة من التسجيلات البئرية مثل المقاومة الكهربية والكثافة والنيترون وأشعة جاما، وتسجيل الرنين المغناطيسى النووى الحديث لأربع آبار للتنمية موزعة فى حقل سيكويا . كما شملت الدراسة مقارنة بين النماذج المختلفة (الماء المزدوج و الأندونسية) لحساب التشبع بالماء للخزان واختيار أنسب نموذج مع عمل مقارنة بين نتائج المحسوبة من التسجيلات البئرية التقليدية والأخرى الحديثة (الرنين المغناطيسى النووي) بالإضافة إلى دراسة العلاقة بين البوتاسيوم والتأثير الكهروضوئى و الثوريوم لمعرفة نوع الطفل الموجود داخل خزان سيكويا وتم أيضا دراسة الاتصال الرأسى والأفقى بين الطبقات ومنسوب الماء فى الخزان من خلال دراسة العلاقة بين العمق والضغط لكل الآبار. ولقد أظهرت النتائج أن قيم التشبع بالماء للصخر المحسوبة من نموذج الماء المزدوج هى الأقرب لقيم التشبع بالماءللصخر المحسوبة من الرنين المغناطيسى النووى حيث تتراوح متوسط قيم التشبع بالماء المحسوبة من التسجيلات التقليدية للآبار بين ٣٨% و ٦٨ % والمسامية الفعالة من ٢٨% إلى ٣٢% بينما متوسط قيم التشبع بالماء المحسوبة من التسجيلات الحديثة تتراوح بين ٣٩% إلى ٧٠ % والمسامية الفعالة بين ٢١% إلى ٢٣% والنفاذية بين ٣٠ إلى ٨٩٠ ميلى دارسى وهذا الاختلاف فى القيم يرجع الى أن التسجيلات البئرية التقليدية تعتمد على نوع الصخر والموائع الموجودة داخله بينما الرنين المغناطيسى النووى يعتمد على الموائع فقط. وقد أوصت الدراسة بحفر آبار تنمية جديدة لاستكمال تنمية الحقل على الوجه الأمثل.

**ABSTRACT:** *This work is devoted to the study of the petrophysical parameters (porosity-permeability- formation water resistivity-hydrocarbon and water saturation-shale content) for Sequoia Pliocene reservoir rocks in Sequoia field in west Nile Delta deep marine concession (WDDM). A suitable model was built for this reservoir using the conventional logging tools (Gamma ray-Density-Neutron-Resistivity) and the new logging tool (Combinable Magnetic Resonance tool "CMR") in 4 development wells.*

*Comparisons between the different saturation models (Dual water and Indonesian) to select the best one applicable for this reservoir, plus comparison between CMR and conventional tools results were done.*

*A study of the lateral, vertical reservoir connectivity and mineralogical identification through pressure plots and Thorium, photo electric effect, and uranium cross plots was done.*

*The results show that average effective porosity calculated from Neutron-Density varies from 28% to 32%, while average effective porosity calculated from CMR using DMR method ranges from 21 % to 23%. The average water saturation calculated from conventional tools (Dual water and Indonesian) ranges from 38% to 68%, while the average water saturation calculated from CMR ranges from 39 % to 70%. The average calculated permeability from CMR using Timur-Coates model varies from 30 to 890 md. On the other hand, the results show that the water saturation from Dual Water model is the closest model to the water saturation calculated from CMR, and this variation is that conventional tools are fluid and lithology dependent, while CMR is only fluid dependent. The study recommended drilling new wells to develop this field.*

## INTRODUCTION

Accurate petrophysical evaluation of deep water channels composed of thin bedded sand-shale sequences is crucial in the economic decision to explore, develop and produce these reservoirs so that a new and conventional logging techniques are used to identify reservoir characteristics accurately and select the best model for this area to determine water saturation, porosity, volume of shale and permeability as there are different saturation models with no precise limitations to use certain model than others, so there should be many researches to help log analysts to choose the most suitable and representative shaly sand model for a certain formation sothat CMR is used with conventional tools as CMR is a Schlumberger tool which sends a permanent magnetic field to polarize the hydrogen protons in a preferred orientation. For these protons to generate a measurable signals , they must be at a condition of resonance which can be achieved with an oscillatory magnetic field and once oscillatory magnetic field is removed signals are generated (resonance) as the exponential decay of this signal is represented by $T_2$ relaxation time which is a function of